Computer Methods and Programs in Biomedicine (2005) **78**, 179—190

ELSEVIER

Computer Methods and Programs in Biomedicine

www.intl.elsevierhealth.com/journals/cmpb

Development of a simulator for radiographic image optimization

Mark Winslow[a], **X. George Xu**[a,b,*], **Birsen Yazici**[c]

[a] *Program of Nuclear Eng. and Eng. Physics, Rensselaer Polytechnic Institute, Troy, NY 12180, USA*
[b] *Department of Biomedical Engineering, Rensselaer Polytechnic Institute, NES Building, Tibbits Avenue, Troy, NY 12180, USA*
[c] *Department of Electrical, Computer, & Systems Engineering, Rensselaer Polytechnic Institute, Troy, NY 12180, USA*

Received 12 October 2004; received in revised form 20 January 2005; accepted 4 February 2005

KEYWORDS
Monte Carlo;
Image simulation;
X-ray

Summary A software package, incorporating two computational patient phantoms, has been developed for optimizing X-ray radiographic imaging. A tomographic phantom, visible photographic Man tomographic phantom (VIP-Man), constructed from Visible Human anatomical color images is used to simulate the scattered portion of an X-ray system using the Electron Gamma Shower National Research Council (EGSnrc) Monte Carlo code. The primary portion of an X-ray image is simulated using the projection ray-tracing method through the Visible Human CT data set. To produce a realistic image, the software simulates quantum noise, blurring effects, lesions, detector absorption efficiency, and other imaging artifacts. The primary and scattered portions of an X-ray chest image are combined to form a final image for future observer studies and image quality analysis. Absorbed doses in organs and tissues of the segmented VIP-Man phantom were also obtained from the Monte Carlo simulations. This paper presents methods of the simulator and preliminary results.

1. Introduction

In the United States, approximately 250 million radiological examinations are performed each year, making diagnostic medical examinations the largest source of man-made radiation exposure [1]. A major goal of radiography is to maximize the amount of diagnostic information while minimizing the radiation exposure to the patient. All radiographic X-ray examinations require the selection of a beam quality (i.e., X-ray voltage and filtration) and X-ray tube output (mA s), which affect both the patient dose and the corresponding image quality. Optimization is difficult because of the following four reasons: (1) the X-ray imaging chain contains a large number of variables associated with X-ray source, patient anatomy, scatter removal grid, and X-ray detector system; (2) diagnostic X-ray examinations involve various body sites and tasks; (3) effective dose is the sole indicator of patient risk but is not obtainable without a whole-body phantom of delineated

* Corresponding author. Tel.: +1 518 276 4014.
E-mail address: xug2@rpi.edu (X.G. Xu).

0169-2607/$ — see front matter © 2005 Elsevier Ireland Ltd. All rights reserved.
doi:10.1016/j.cmpb.2005.02.004

organs; (4) perception plays a key role in evaluating image quality, which needs to be related to radiologist performance. At the core of the problem is the lack of a suitable simulator capable of interlinking image quality and patient dosimetry. Although different aspects of this problem have been previously studied [2,3], at this time, there is no simulator that will allow for such a complicated optimization process to be performed. To this end, we have developed the virtual photographic and radiographic imaging simulator (ViPRIS) that has the potential to meet our needs.

At the core of this simulator are the image sets that have been made available to the public by the United States Nation Library of Medicine's Visible Human Project (VHP). The VHP was conducted to create digital anatomical data for adult male and female by obtaining transverse CT, MR and cryosectional images of representative male and female cadavers. For our project, ViPRIS utilizes two sets of anatomically identical datasets: color cryosectional photographs and CT scan images [4]. ViPRIS contains an image projection phantom constructed from the CT data set to simulate the primary X-rays. Scattered X-rays are simulated using the visible photographic Man tomographic phantom (VIP-Man) previously constructed from segmented color cryosectional photographs of the VHP (as discussed in more detail below). The two phantoms are of identical anatomy, allowing study of patient dose and production of radiographic images simultaneously. ViPRIS is very flexible and allows for the adjustment of different parameters. Nodules can be embedded in ViPRIS to evaluate the threshold of detectability at different locations. The user is permitted to specify different grid filtering parameters and the detector efficiency. A simple user-friendly software interface permits an observer to investigate the relationship among nodule detection threshold, nodule characteristics, patient dose, detector efficiency, and X-ray beam settings.

2. Background

2.1. Prior work: the VIP-Man model to compute radiation doses

The VIP-Man model was originally developed from the VHP image data to calculate radiation doses to an adult male [5]. Image data from the VHP include four sets of images of two cadavers [4]. The male cadaver weighed 90 kg and was 186 cm tall. CT, MRI, and X-ray images were first obtained of the fresh body. The body was then frozen to allow 1-mm thick slices to be removed from head to toe for cross-sectional color photographs. At the end of the VHP, a total of 1878 transverse color photographs were obtained and segmented to identify up to 1400 organs and tissues of interest for the male cadaver to form a digital atlas of what was called the ''Visible Man.'' At Rensselaer, segmentation and classification were performed to finally adopt 72 radiosensitive organs and tissues for radiation dosimetry studies [5]. A sample slice of the VHP man cryosectional photos, the corresponding segmented VIP-Man image slice, and the corresponding CT slice are provided in Fig. 1. Values of tissue densities and compositions for radiation dosimetry calculations were based on those recommended in ICRP 23 [6]. The original voxel size of the VIP-Man model is 0.33 mm $\times$ 0.33 mm $\times$ 1 mm and the whole body is represented by 3,384,606,720 voxels. The VIP-Man model has been implemented into Monte Carlo simulation codes to study radiation doses of an adult male exposed to various external and internal sources [7—10]. Complete listing of papers related to the VIP-Man model can be found at RRMDG.rpi.edu.

2.2. Modification of the VIP-Man model for this study

In order to reduce the computational time, a simpler version of the VIP-Man model with a voxel size of 1 mm $\times$ 1 mm $\times$ 1 mm was utilized for this study. In X-ray examinations, a patient often raises the arms to expose the chest area. For this reason, the arms of the original VIP-Man model were removed to more realistically represent a patient undergoing an X-ray examination. Approximately, 200 slices of the VHP transverse images of the upper arms were manually edited using a commonly available commercial imaging software package. In the upper arm region, the arms were in contact with the main body. Anatomical landmarks were used to decide where to delineate the boundary. After a section of arm was removed, a layer of skin with proper thickness was added to the main body. The lower arms and hands were removed from the body by using a custom C++ code that utilized an object size filter to automatically identify and remove objects not connected to the main body. We used the code to process an additional 250 slices. All modified slices were manualy viewed and verified slice by slice prior to our Monte Carlo calculations. Three-dimensional surface renderings of the armless VIP-Man model can be seen in Fig. 2.

A total of 72 separate organs and tissues were tagged with information on chemical composition,

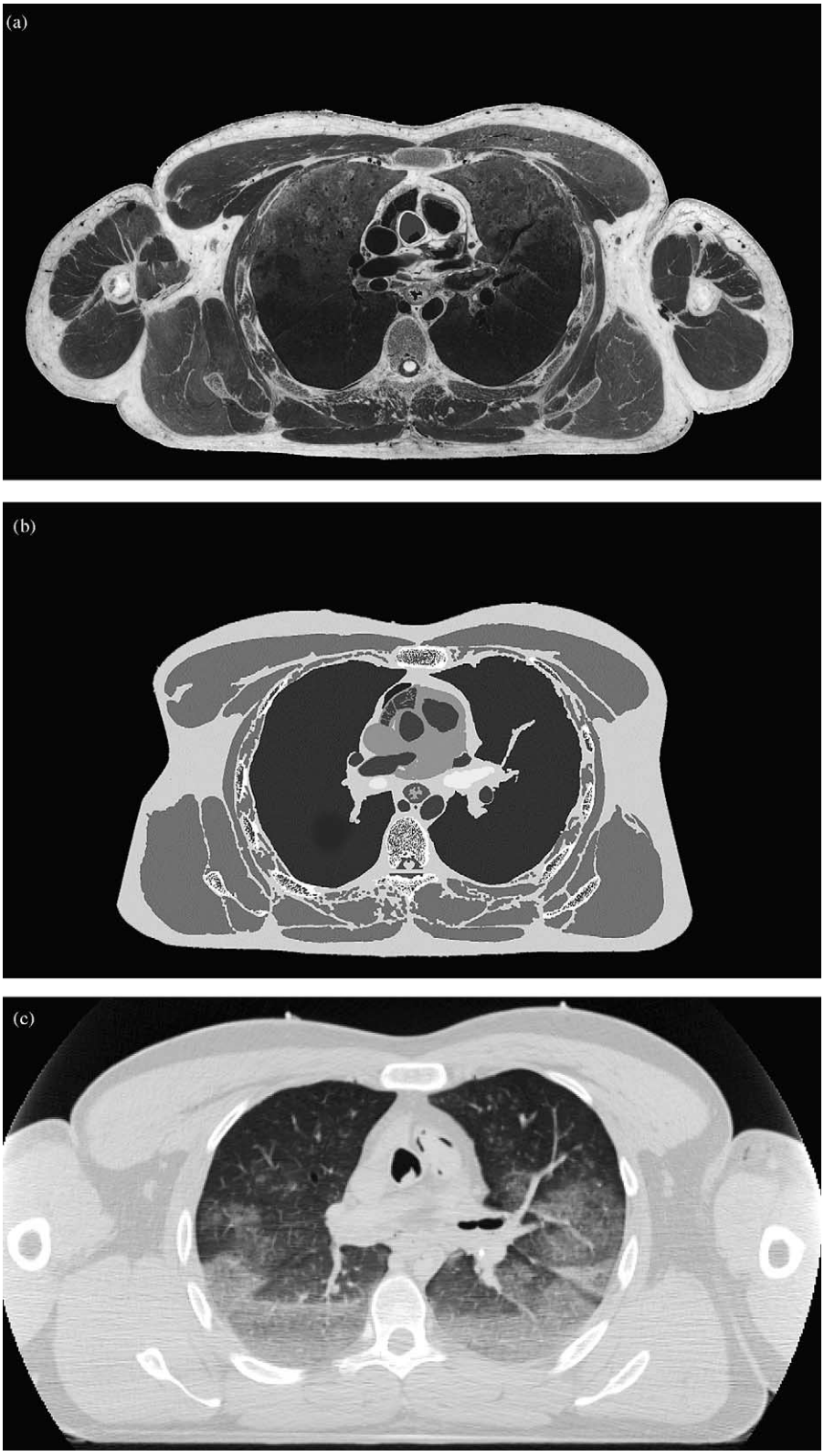

Fig. 1 Gray scale image of the (a) original cryosectional image of the male Visible Human Project and (b) corresponding slice of the segmented VIP-Man Phantom, and (c) image of the corresponding CT scan slice of the male Visible Human Project.

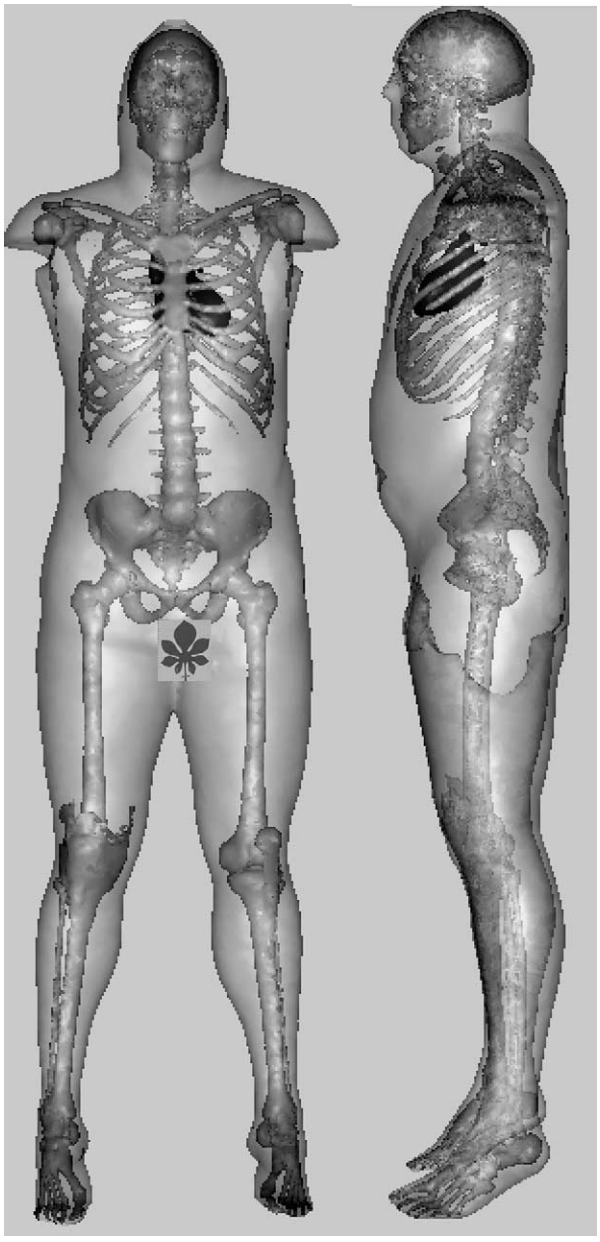

Fig. 2 Surface rendering of the VIP-Man tomographic model with the skin, heart, and bone displayed.

density, and location for Monte Carlo simulations in two codes: MCNP and Electron Gamma Shower National Research Council (EGSnrc) [11,12]. The EGSnrc code is used in this study to calculate organ doses as well as the scatter images, but a cross-check with the MCNP code was made at an early stage of the study to verify the geometry definitions of the VIP-Man. Because VIP-Man is defined by an extremely large number of voxels, a look-up table algorithm was developed to reduce the burden on computer random access memory by compressing the image data in EGSnrc.

2.3. Related work and lessons learned

Lazos et al. at University of Patras in Greece and Sandborg et al. at Linköping University in Sweden have studied image optimization using computer models of dosimetry and imaging, respectively [2,3].

The group from University of Patras has developed software that produces images based on a simulated X-ray system. The system includes several modules including the following: Monte Carlo modeling of the particle beam with variable spectrums (kVp); grid transmission rates; image formation; voxel dose calculations. The Patras group's simulator is a significant advancement in computerized simulation of radiography. However, the objective of our software, ViPRIS, is to optimize the imaging chain by identifying ways to maintain satisfactory image quality while minimizing the effective dose to the patient. Different tissues within the body have different weighting factors with regard to radiation risk [13]. Without a phantom containing segmented and defined organs such calculations have to rely on conversion coefficients developed for an average person, and not the specific person being studied. According to Wise et al. [14], variation of patient size, sex, field size, and field position can lead to significant variation of effective dose per kerma area product by up to a factor of two. The VIP-Man phantom provides an ideal opportunity to develop a well-defined database of organ doses for a specific individual. When a small amount of radiation (low fluence) is used to produce an image, the quantum (statistical) noise in the image is the predominating factor that degrades image quality. This effect can be seen in videos obtained using night vision technology when there is little light, or low photon fluence. Fig. 6a contains a low fluence image. When an image is degraded severely by quantum noise the radiologist's ability to detect lesions within the radiograph is limited. Our effort includes the addition of a quantum noise model. Originally we attempted to produce images solely using Monte Carlo techniques. We discovered that the computing time required to produce an adequate image was not practical. Therefore, we adopted the approach proven by the Patras group of creating two sub-simulation systems. Adopting the split system approach developed by the Patras group proved invaluable and allowed for the development of the simulator.

The group from Linköping University has developed a software package designed to calculate the contrast of veins and arteries within a tomographic phantom [2]. The Linköping group used a phantom developed earlier at Yale University for nuclear

medicine applications [15]. The phantom was built from CT images for head—torso region of the body with only a small number of tissue types. The resolution of the images used to construct the phantom were not as fine as those from the VHP. The mathematical simulations conducted by the LinkÖping group proved that human tomographic phantoms could be used for studying image quality characteristics. We wish to advance the technique by using the more detailed VIP-Man phantom with more tissue types and by simulating actual radiographic images for use in observer studies.

3. Design considerations

The objective of ViPRIS is to produce simulated radiographs of reasonable quality, using variable settings, which contain simulated lesions of various sizes, and locations. The simulated radiographs could then be used in future image quality analysis studies. In order to ensure the clinical applicability of the simulated images, we have collaborated with experienced radiologists and medical physicists at State University of New York, Upstate Medical University.

When the simulator was first conceived in 2001, we produced images solely using the VIP-Man phantom. The images were blocky and did not contain full anatomical details. This was because the lungs in the VIP-Man were assigned a uniform density during the segmentation and organ delineation process for calculating average organ doses. While this segmentation was adequate for radiation protection dosimetry and Monte Carlo modeling purposes, it did not contain subtle anatomical details about the lungs. The lungs on the initial images had a single solid gray scale value. As a crosscheck, we compared the ViPRIS images to the VHP chest X-rays. Being engineers, we had thought that the images were of good quality, until the consulting medical physicists and radiologists indicated otherwise. In the radiologists' experience, normal anatomy significantly confounds the detection of lesions. If, for example, a lesion is present within a patient's lung near veins and other structures, it becomes much more difficult to detect. By simulating the lungs as a continuous tissue type as we did initially, the detection process would have been unrealistically too easy for observers. The observer studies therefore would have indicated a much lower threshold for detection than would have been obtained in a real patient. It was at this point that we adopted the split approach in using two phantoms for two different purposes. The formation of simulated chest X-ray images has been since divided into several phases as detailed below. Images formed in such a way were satisfactory to the radiologists and medical physicists.

4. System description

4.1. Stages of image formation and optimization process

Optimization of the radiography process occurs using three modules. ViPRIS is used to produce realistic chest X-ray images and represents the first module. The second module is the VIP-Man phantom and the dosimetry calculations within EGSnrc. The third module is simulated observer studies using Hotelling statistics and an analysis program within the MATLAB software program. The observer studies module will be discussed as part of our future work.

4.2. Formation of the X-ray image

The geometry used for formation of the image can be seen in Fig. 3. ViPRIS simulates X-ray projection in three phases. First, for a given X-ray tube setting, ViPRIS calculates the primary X-ray intensity (i.e., transmitted X-rays) by tracing each X-ray through the image projection phantom. ViPRIS then scales and calculates the scattered X-rays based on stored data files from pre-generated Monte Carlo simulations. The scattered data set is smoothed to remove excess noise cause by statistical variations inherent in Monte Carlo simulations. Each data set is modified based on the specified detective quantum efficiency. Quantum noise is added to the primary and scattered images. Finally, the two images are combined to form the simulated radiograph. The details of each step of the process are given below.

4.2.1. Primary X-ray image

The primary X-ray image is formed by photons that transmit through the patient anatomy without interactions. The number of transmitted photons is readily obtainable from attenuation coefficients of the associated tissue volume. Visible Human CT images are useful because they contain the electron density of each tissue slice and can be converted into attenuation coefficient data using Equation (1).

$$\mathrm{HU}_x = 1000\frac{\mu_x - \mu_w}{m_w} \tag{1}$$

$$I = I_0\, e^{-t\Sigma\mu} \tag{2}$$

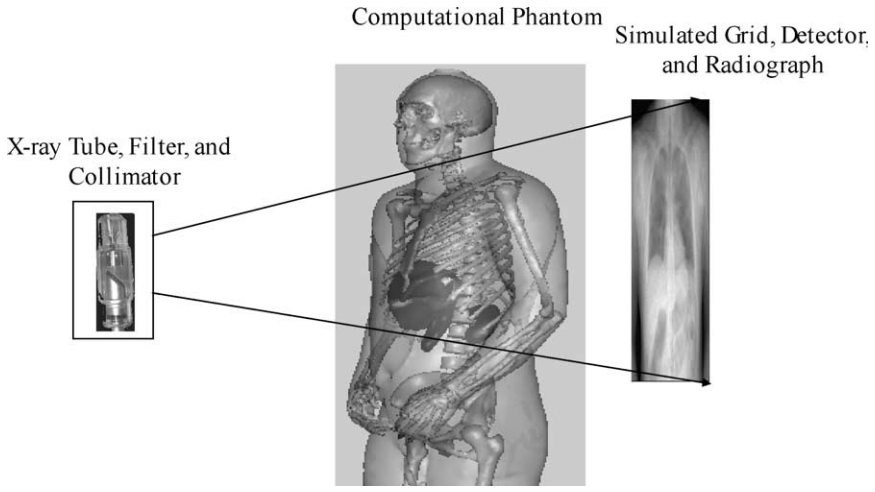

Fig. 3 Radiographic imaging chain containing the ViPRIS computational phantom. The simulated image receptor will have transmitted and scattered photons.

where HU_x is the Hounsfield Unit value of voxel x, μ_x the linear attenuation coefficient of the material of voxel x, and μ_w is the attenuation coefficient of water. I in Equation (2) is the number of photons that transmit through the body along the X-ray beam, where I_0 is the number of photons incident on the patient along the path from the source to the detection pixel, t the voxel dimension in the anterior/posterior direction, and μ is calculated by ViPRIS from the Visible Human CT data set for every pathway/pixel. The attenuation coefficients are summed along the path length, as illustrated in Fig. 4. X-ray tube output (mAs) determines the number of X-ray photons to be emitted from the tube, and is simulated by I_0 as specified by the user.

The Visible Human CT data set does not contain lesions in the chest. To simulate lesions, ViPRIS replaces attenuation coefficients of certain voxels within the selected chest region of the CT with those of lesions. The software allows a user to select a variety of lesion geometries and compositions in the form of a lesion HU. For example, a fatty lesion will have a lower HU than a calcified lesion.

$$I = I_o e^{-(\mu 1+\mu 2+\ldots)t}$$

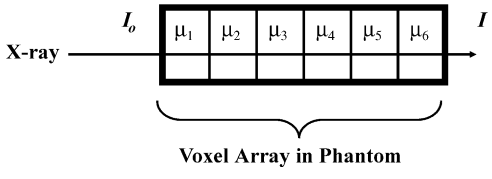

Fig. 4 Intensity of the transmitted photons is determined by the total attenuation coefficients of the voxels an X-ray transverses.

4.2.2. X-ray scattering image

When an X-ray photon enters the patient body, there is a probability that an X-ray may undergo scattering from the path towards the film or detector grid and will add a random background noise to the primary image. A critical part of increasing the signal-to-noise ratio within a radiographic image is removing the scattered signal from the final image receptor. Anti-scatter grids only attenuate, and do not totally block, the scattered X-rays. Because the scatter and primary portions of an image are combined on a film or detector, the pattern at which a scattered photon contributes to a radiograph is still not fully characterized. Monte Carlo techniques are ideally suited for modeling this random process. The Monte Carlo computer code EGSnrc is used in ViPRIS to simulate the detailed photon interactions in the phantom. The scattered portion is recorded for later use. This process is extremely time consuming because the probability of Compton scattering is relatively small for X-rays and a large number of particle histories are necessary to reduce the statistical uncertainty inherent in the Monte Carlo method. To further reduce the statistical uncertainty (motel or noise) each data set are soothed or denoised using a 24×24 boxcar filter. Selection of the 24×24 boxcar smoothing filter was based an experiment during which several smoothing filters were examined. Smaller filters did not provide enough of a denoising effect and larger filters generated too much blurring. The error introduced by the 24×24 smoothing filter is minimal because the scatter portion of an image is a general fog without specific anatomical detail that is superimposed over the entire image. The filter has a width of approximately 2 cm. The lungs were the only anatomical

landmarks that were identifiable with any of the filters examined. To ensure that we have used the proper number of particles required for a reasonable image, we ran an experiment on a sub section of the phantom's lung/chest region. We conducted several simulations of varying fluences ranging from 1 to 1000 million on a section of the chest. Because of the focusing effect of reducing field size, this was equivalent to running approximately 7 billion particles on the entire phantom. The 1000 million run was selected as our gold standard. A comparison was made between each of the lower fluence runs to see how closely they resembled the high fluence image. From this experiment, we determined that 100 million particle histories for the higher energy simulations (>40 keV) and 1 billion particle histories for the lower energy simulations provided an accurate representation of the scatter portion of the image. Because the X-ray scattering process is extremely inefficient, the Monte Carlo simulations are time consuming. Using our computational hardware system, the image data files required approximately 6 weeks to produce.

4.2.3. Formation of the final image

Once the primary and scatter images are calculated, ViPRIS accounts for various imaging components detailed below and forms a final image. Prior to any operations the scatter data are scaled to match the fluence specified by the user.

Quantum noise within an imaging system is a normal distribution or a Poisson distribution. With an adequate sample size a Gaussian distribution is representative. ViPRIS uses a Box—Muller approximation of a Gaussian distribution to add simulated quantum noise to the primary and scatter image data [16]. The square root of the number of photons incident on a pixel is used to simulate the standard deviation of noise as governed by Gaussian statistics. Equation (3) shows how a Box—Muller distribution is generated. Variables x and y are random numbers uniformly distributed over the interval [0, 1]. n Is the resultant Gaussian random distribution with a zero mean and standard deviation of one. The resulting n is multiplied by the assumed standard deviation and added to each pixel count.

$$\begin{aligned} f(x) &= \sqrt{-\ln(x)} \\ g(y) &= \sqrt{2}\cos(2\pi y) \\ n &= f(x)g(y) \end{aligned} \tag{3}$$

Because the quantum absorption efficiency (detection efficiency) of the detector is not unity, the user specified efficiency is used to modify the number of particles detected in all pixels. This allows for the simulation of any detector as well as X-ray system.

To convert the photon fluence of the primary image into energy fluence the number of surviving particles in each pixel (I from Equation (2)) is multiplied by the user specified energy. For the scattered portion, the same procedure is followed; however, the average scatter particle energy is used.

To combine the scatter and primary portions of the radiograph the specifications of the user-defined grid are utilized. ViPRIS simulates the presence of a grid by allowing the user to specify the transmission percentages of the primary and scattered image. Any grid can be simulated using Bucky factors and scatter to primary ratio data specified by grid manufacturers. The default grid is a standard 10:1 with a transmission rate of 65% primary and 5% scatter. For example, when the user specifies a 0% transmission of the primary photons, the primary image is completely removed and the scattered image is displayed. Conversely, when a 0% transmission of the scattered photons is selected, the scattered image is removed and the primary image is displayed.

The response curve of film is an elongated S shape with a log linear useful region, while modern digital detectors have a nearly linear response curve across the entire dynamic range [17]. Since ViPRIS is designed to simulate the more modern digital detector system, the log of the energy fluence is assumed to be log linear. The data set is then scanned for the lowest and highest numbers. The lowest log energy fluence is then subtracted from each data point. A new maximum is calculated and divided by 255. The data are then converted into a gray scale value between 0 and 255.

4.3. Calculation of organ doses for risk assessment

Prior to the development of the full ViPRIS system, we tested using the VIP-Man phantom to evaluate the doses received by patients during several common radiographic evaluation procedures [18]. We discovered the number of particle histories required for adequate statistics needed for effective dose calculations were approximately 100 times less than those required for production of the scatter image.

When the photon fluence used to create a radiographic image is increased, the number of photons that reach the X-ray film or digital X-ray sensor will increase, leading to an improved signal-to-noise ratio. Unfortunately, increasing the fluence will simultaneously increase the radiation dose to the patient. ViPRIS is designed to allow the user to specify how many particles are projected on each

image pixel (I_0). When a small number of photons are specified, the projected image is grainy (noisy) and it is difficult to observe fine details. During the optimization process, a ViPRIS user can observe how the quality of an image changes with different photon fluencies. Our objective is to find the point were adequate images are produced with the minimum dose.

Organs receive X-ray doses from secondary electrons resulting from photoelectron absorption and Compton scattering. During the formation of the scatter profile the EGSnrc code tracks the energy deposition in each of the major organs of the VIP-Man model. The mean absorbed dose in an organ or tissue (D_T) is calculated as the total energy deposited in organ T divided by the organ mass. The equivalent dose (H_T) in organ T is calculated by multiplying the mean absorbed dose by the radiation-weighting factor, w_R, which is unity for photons and electrons. Since the same equivalent dose value can cause different risk in different organs or tissues, a tissue-weighting factor (w_T), has to be applied to

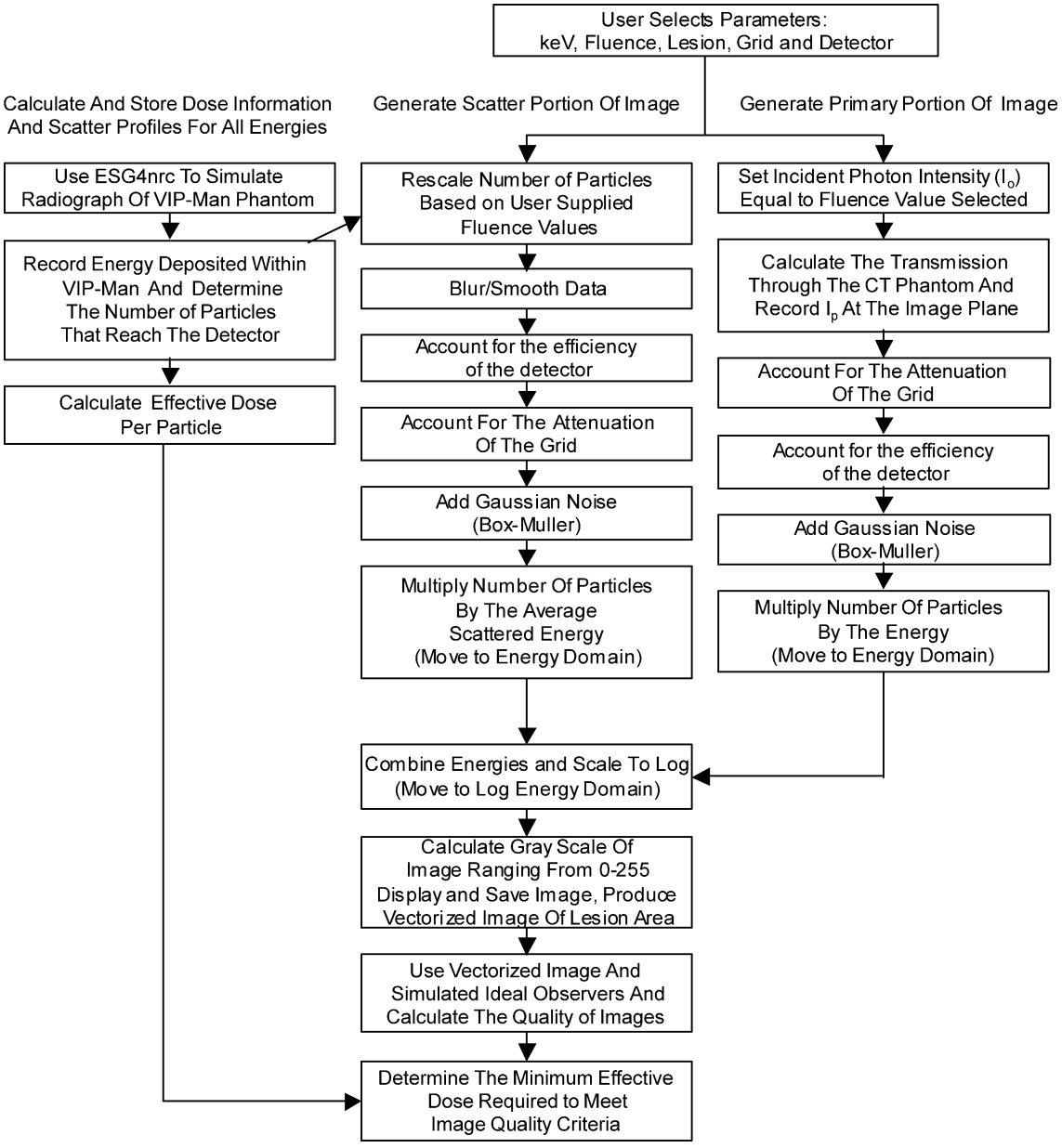

Fig. 5 Flow chart of optimization process, spilt into four sections: Monte Carlo data generation and effective dose calculation (left), development of the scatter portion of the image from the Monte Carlo data profile (upper center), development of the primary portion of the image from the ray tracing algorithm (right), and analysis of the generated images and determination of lowest dose setting (lower center).

yield the total risk, in terms of effective dose (E) using Equation (4) [13].

$$E = \sum_T w_T H_T \quad (4)$$

Twelve critical organs/tissues and their weighting factors are explicitly recommended by the ICRP. The bone surface, which is in the scale of $\sim$10 μm, is too small to be defined in VIP-Man. Consequently, the dose to bone surface was substituted with the dose to bone, as in all such calculations. The testis (only one remained in the Visible Man) within the VIP-Man model was used to represent gonads. A thin layer of fat tissue around chest level is used as male breast. Ten more organs and tissues are included in the remainder group of organs which together shares a total tissue weighting factor of 0.05. In a later ICRP Publication [19], upper large intestine was combined to the critical organ, colon. Thus, the VIP-Man has only eight organs in the ''Remainder'' group according the ICRP definitions (no female organs in VIP-Man, e.g., uterus).

Monoenergetic photons were considered in ViPRIS for dose calculations. The user specifies the energy to be used for each simulation. For each pregenerated scattered image there is a corresponding dosimetry data set. When the scatter data file is loaded the associated dosimetry data set is also specified. The data set contains conversion factors for effective dose per particle at the specified energy. Since the user specifies a fluence to be simulated an effective dose is calculated by multiplying the dose conversion factor by the fluence.

4.4. Hardware and compiler information

Scatter images were generated using EGSnrc on a computer using a 1.6 GHz Pentium 4, 512 MB of RAM, running Linux. ESG4nrc uses a MORTRAN compiler. A total of 100 million particle histories were simulated for energies between 40 and 150 keV, while 1 billion particle histories were simulated for 30 and 35 keV. The 1 billion particle runs required approximately 2 weeks while the 100 million particle runs required approximately 1.5 days. Primary image formation and merging of the scatter and primary images took place in a C++ code running on another computer utilizing Windows XP. Energy or particle counts per pixel are represented by large two-dimensional float arrays, 440×494. A flow chart of the basic operations can be seen in Fig. 5.

Because we wished to simulate many different radiographs, the scatter image was saved and scaled depending on the fluence desired within each simulation. Development of each simulated image using the C++ portion of the code takes approximately 3 min. The scatter image does not

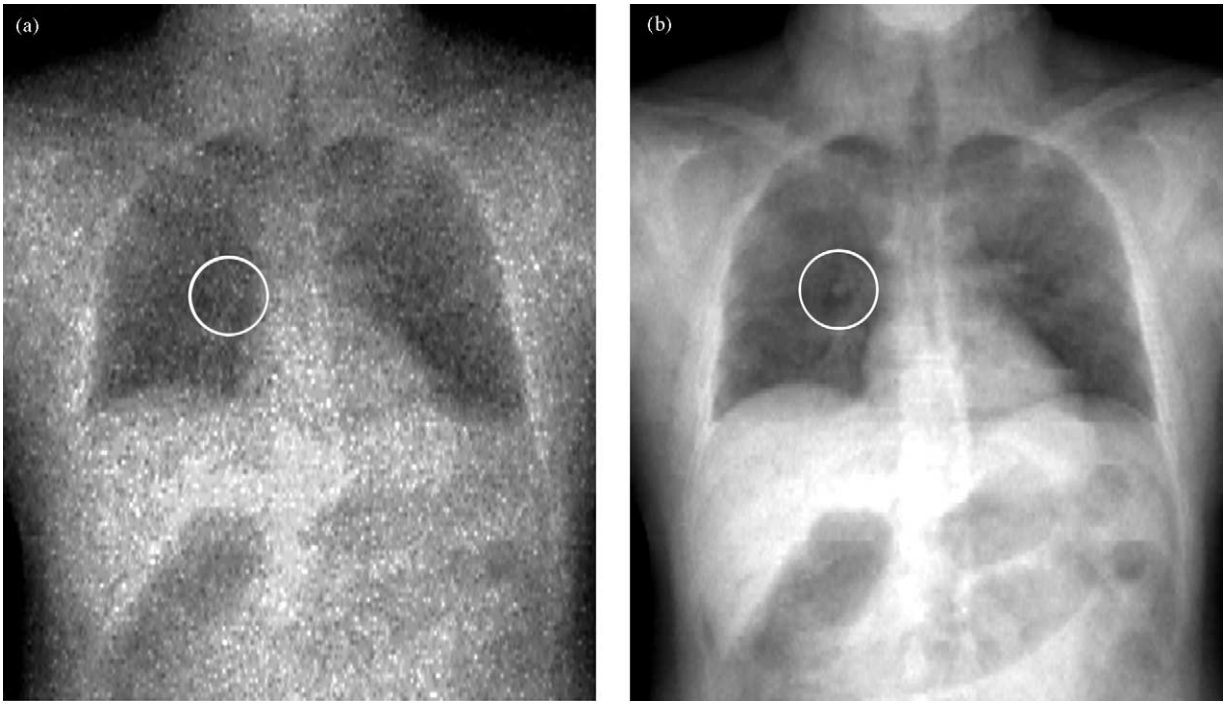

Fig. 6 Simulated primary chest X-ray images for 50-keV X-rays with a lesion (highlighted by the circles) for different photon fluence: (a) at relative fluence of 1, the lesion is not visible and (b) at relative fluence of 100, the lesion is visible.

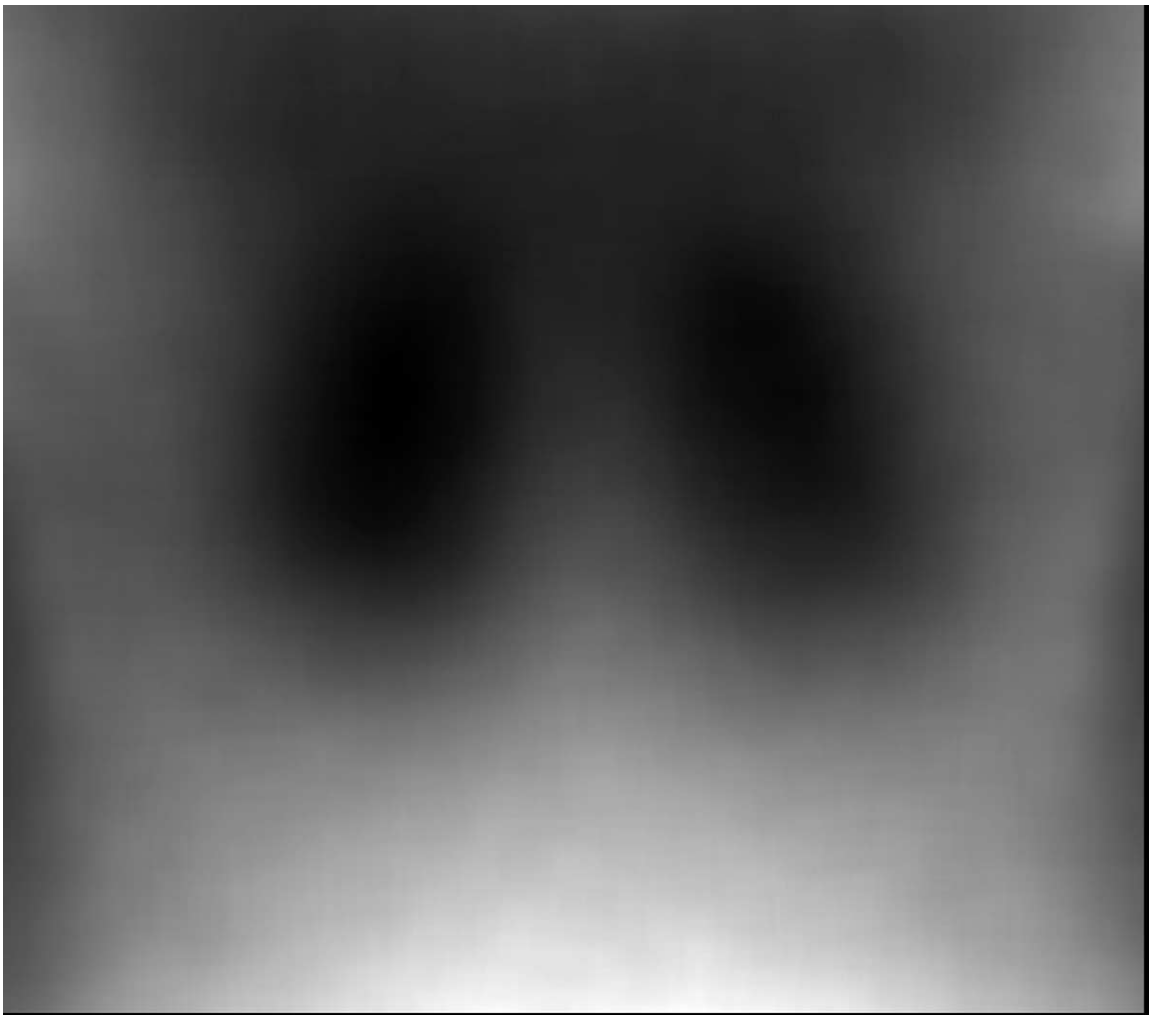

Fig. 7 Scattered 50-keV X-rays simulated using VIP-Man tomographic phantom and Monte Carlo method. One-hundred million particles were simulated.

contain a lesion. However, the scatter image is a general fog and the impact of not having a small lesion (1 cm $\times$ 1 cm) within the VIP-Man phantom is minimal. By only placing lesions within the primary imaging code we have been able to simulate a multitude of different fluence and lesion combinations in a single afternoon. Using a pure Monte Carlo approach would have required several days to calculate each data point.

5. Status of work

Fig. 6 shows preliminary images we have obtained using the image projection phantom for the primary transmission at 50 keV, at two different levels of radiation exposure. The images in Fig. 6 also show a circular mass lesion that has been inserted into the right lung. It can be seen that image quality improves as the fluence increases from Fig. 6a and b due to the 10-fold reduction in the level of quantum mottle (noise) (caused by a 100-fold increase in photon fluence); the added lesion is essentially invisible in Fig. 6a, but is readily visible in Fig. 6b. In generating these types of images, we have total control over both the lesion characteristics (size, shape, and composition) and the lesion location.

Fig. 7 contains a preliminary image of the scattered 50-keV X-rays. It can be observed from the image that the scattered X-ray energy deposition has a non-uniform pattern throughout a radiograph.

Effective dose and organ doses have been calculated in a previous paper for photons incident for several views and charted with regard to energy imparted [17]. The feasibility of ViPRIS in calculating effective doses of a patient has been demonstrated, and we will extend our calculations to include all X-ray energies and fluences. Once simulations are completed, this work will result

in a thorough database for organ doses from chest X-ray examinations.

6. Lessons learned

The simulator has been in development for over a year. During that time, we attempted to generate images using a combination of techniques including pure Monte Carlo techniques. When the system was modeled using pure Monte Carlo techniques the simulation took several days, and the resulting image was unrealistic and only contained bones. Details of the lungs, stomach, and heart could not be observed. We then tried to simulate the radiography using a pure ray-tracing algorithm. The simulated radiographs we obtained were not realistic enough because they did not contain adequate anatomical variation. Lung tissue contains many variations. The VIP-Man phantom simulated the lungs as a uniform tissue. Small lesions can hide inside the subtle variations caused by anatomy.

By splitting the simulation into Monte Carlo and a primary image analysis portions, we reduced the runtime considerably. Previous work ran a Monte Carlo simulation each time a single parameter was changed. Therefore, each simulation took many hours and multiple simulations were required to reduce quantum noise. By running a large number of particles and saving the data file, statistical noise has been significantly reduced. Once a data file has been generated running a simulation within the C++ program only takes a few minutes. These innovations allow the user to generate many simulated images in a few hours.

7. Future plans

7.1. Image quality analysis

In the future, we will demonstrate that the ViPRIS simulator can be used for chest X-ray system optimization given a specific diagnostic task, such as tumor diagnosis or staging. We will couple the ViPRIS with a simulated model observer to quantify the quality of the images produced with respect to tumor detectability. Measures of image quality with respect to tumor detection have been studied extensively by other groups [20,21]. Our plans are to build on their work. We are in the process of evaluating the use of several observer models including Hotelling observer, channelized Hotelling observer, and a non-prewhitening matched filter with an eye filter. We have developed a program in MATLAB to implement and test the use of these simulated observers and will be publishing our findings in the near future.

7.2. Conclusion

We have constructed ViPRIS to study optimization of the X-ray imaging chain. The tomographic phantoms constructed from Visible Human anatomical color images and the computed aided tomography data set combined with the ESGnrc Monte Carlo code and our custom ray tracing algorithm are ideal for simulating a true radiograph. Quantum noise and blurring effects are the key ''degradation'' components, which are needed to form a final chest X-ray image that is realistic for use in radiological research. Development of ViPRIS also permits accurate organ doses and effective doses to be obtained from validated Monte Carlo simulations. In the future, we will automate the X-ray image production and perform observer studies using simulated observers. Such studies will include a range of nodule morphology (spherical, lobulated, and speculated) and investigate detection performance in different types of anatomic backgrounds. ViPRIS is expected to be a powerful tool to study the intricate relationship between dose and image quality in radiological imaging.

Acknowledgments

We wish to thank Dr. Walter Huda, Dr. Kent Ogden, and Dr. Ernest Scalzetti of the Department of Radiology, State University of New York, Upstate Medical University, for their guidance and input on the clinical realism of the simulator.

References

[1] United Nations Scientific Committee on the Effects of Atomic Radiation (UNSCEAR). Sources and Effects of Ionizing Radiation. 2000 Report to the General Assembly, UN, New York, 2000.
[2] M. Sandborg, G. McVery, D.R. Dance, G.A. Carlsson, Schemes for the optimization of chest radiography using a computer model of the patient and X-ray imaging system, Med. Phys. 28 (2001) 2007—2019.
[3] D. Lazos, K. Bliznakova, Z. Kolitsi, N. Pallikarakis, An integrated research tool for X-ray imaging simulation, Comput. Methods Prog. Biomed. 70 (3) (2003) 241—251.
[4] V.M. Spitzer, D.G. Whitlock, Atlas of the Visible Human Male, Jones and Bartlett Publishers, 1998.
[5] X.G. Xu, T.C. Chao, A. Bozkurt, VIP-Man: an image-based whole-body adult male model constructed from color pho-

tographs of the visible human project for multi-particle Monte Carlo calculations, Health Phys. 78 (5) (2000) 476—486.
[6] International Commission on Radiological Protection. Report of the Task Group on Reference Man, vol. 23, Pergamon Press, ICRP Publication, Oxford, 1975.
[7] T.C. Chao, X.G. Xu, Specific absorbed fractions from the image-based VIP-Man body model and EGS4-VLSI Monte Carlo code: internal electron emitters, Phys. Med. Biol. 46 (2001) 901—927.
[8] T.C. Chao, A. Bozkurt, X.G. Xu, Conversion coefficients based on VIP-Man anatomical model and EGS4-VLSI code for monoenergetic photon beams from 10 keV to 10 MeV, Health Phys. 81 (2001) 163—183.
[9] T.C. Chao, A. Bozkurt, X.G. Xu, Dose conversion coefficients for 0.1—10 MeV electrons calculated for the VIP-Man tomographic model, Health Phys. 81 (2000) 203—214.
[10] A. Bozkurt, T.C. Chao, X.G. Xu, Fluence-to-dose conversion coefficients based on the VIP-Man anatomical model and MCNPX code for monoenergetic neutron beams above 20 MeV, Health Phys. 81 (2001) 184—202.
[11] J.S. Hendricks, MCNP—A General Monte Carlo N-Particle Transport Code, LA-12625-M, Version 4B, Los Alamos National Laboratory, 1997.
[12] W.R. Nelson, H. Hirayama, D.W.O. Rogers, The EGS4 Code System. Stanford Linear Accelerator Center, SLAC-265-UC-32, 1985.
[13] International Commission on Radiological Protection (ICRP), 1990 Recommendations of the ICRP, Ann. ICRP 21, numbers 1—3, 1991, Publication 60.
[14] K. Wise, M. Sandborg, J. Persliden, Alm Carlsson G sensitivity of coefficients for converting entrance surface dose and kerma-area product to effective dose and energy imparted to the patient, Phys. Med. Biol. 44 (1999) 1937—1954.
[15] I.G. Zubal, C.H. Harell, Voxel based Monte Carlo calculations of nuclear medicine images and applied variance reduction techniques, Image Vision Comput. 10 (1992) 342—348.
[16] G.E.P. Box, M.E. Muller, A note on the generation of random normal deviates, Ann. Math. Stat. 29 (1958) 610—611.
[17] A. Wolbarst, Physics of Radiology, Medical Physics Publishing, Madison Wisconsin, 2000.
[18] M. Winslow, W. Huda, X.G. Xu, T.C. Chao, C.Y. Shi, K.M. Ogden, E.M. Scalzetti, Use of the VIP-Man Model to calculate energy imparted and effective dose for X-ray examinations, Health Phys. 86 (2004) 174—182.
[19] International Commission on Radiological Protection (ICRP), Human Respiratory Tract Model for Radiological Protection, Pergamon Press, Oxford, Ann. ICRP, vol. 24, numbers 1—3, 1994, ICRP Publication 66.
[20] A.E. Burgess, Comparison of receiver operating characteristic and forced choice observer performance measurement methods, Med. Phys. 22 (1995) 643—655.
[21] H. Barrett, K. Myers, Foundations of Image Science, Wiley/Interscience, October 2003.